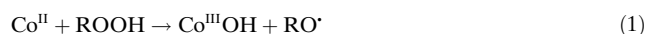


Insights into the Cobalt(II)-Catalyzed Decomposition of Peroxide

Eyal Spier, Ulrich Neuenschwander, and Ive Hermans*

The homolytic activation of alkyl hydroperoxides by cobalt complexes plays an important role in several large-scale oxidation processes such as the autoxidation of cyclohexane (6×10^6 tonnes per year).^[1] This process takes place in two separate steps.^[2] In a first autoxidation step, the substrate is subjected to a radical chain autoxidation, yielding an oxygenate mixture, which contains mainly hydroperoxide, alcohol, and ketone, amongst several by-products.^[3] In a subsequent step, a soluble cobalt(II) complex is added to convert the hydroperoxide to additional alcohol and ketone through radical Fenton chemistry (so-called deperoxidation step). Despite the importance of this chemistry on a large-scale, the elementary reaction steps are still not fully established, and several observations cannot be explained by textbook mechanisms [Reactions (1) and (2)].



Irreversible catalyst deactivation, as well as a maximum in the deperoxidation rate as a function of the cobalt concentration are two important aspects that are not yet understood. Herein, the deperoxidation reaction is investigated by a combination of techniques to gain insight in the elementary reaction steps.

A first observation is the difference in the performance of cobalt(II) acetylacetonate ($\text{Co}(\text{acac})_2$) and cobalt(II) octoate ($\text{Co}(\text{oct})_2$; octoate = 2-ethylhexanoate; Figure 1). Although both catalysts tend to deactivate (first-order kinetic plots deviate from linearity), the octoate complex is much more active and less susceptible to deactivation (i.e., a higher end conversion can be reached). The pseudo-first-order deperoxidation rate constant (k_{obs}) is determined from the initial slope of the plots in Figure 1. The dependence of k_{obs} on the $\text{Co}(\text{acac})_2$ concentration is displayed in Figure 2 for two different peroxide concentrations, and in the presence of the radical trap 2,6-di-*tert*-butylcresol. First-order behavior in cobalt is only observed at low catalyst loadings. At higher catalyst concentrations, k_{obs} features a maximum as a function of the cobalt loading. This observation points towards an

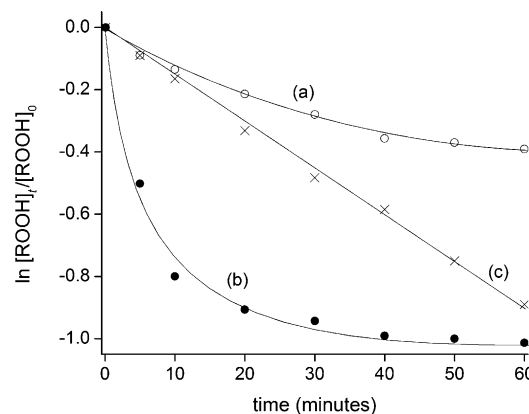


Figure 1. First-order ROOH decay plot at 40°C under the influence of 100 μM $\text{Co}(\text{acac})_2$ (a), $\text{Co}(\text{oct})_2$ (b), and 0.75 wt % $\text{Co}/\text{Al}_2\text{O}_3$ (c); $[\text{ROOH}]_0 = 20 \text{ mM}$.

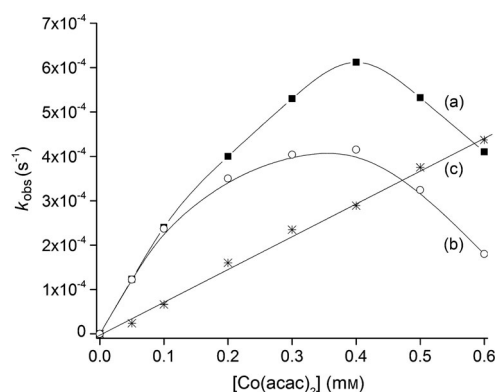


Figure 2. Pseudo first-order deperoxidation rate constant k_{obs} at 40°C as a function of the $\text{Co}(\text{acac})_2$ concentration in the absence (a, $[\text{ROOH}] = 20 \text{ mM}$); b, $[\text{ROOH}] = 50 \text{ mM}$) and presence (c, $[\text{ROOH}] = 20 \text{ mM}$) of the radical trap 2,6-di-*tert*-butylcresol (20 mM).

inhibition mechanism that is (at least) second-order in cobalt. Indeed, earlier it has been proposed that this inhibition could be caused by the trapping of active cobalt species by ROO^{\cdot} radicals [Reaction (3)].^[1] However, if that reaction was highly



exothermic, the catalyst would only be able to perform a single turn-over, in disagreement with our observations. If the $\text{Co}^{\text{III}}\text{OOR}$ bond was weak, an equilibrated trapping would be established. This could at most explain a leveling-off in the reaction rate, but not a maximum. The fact that k_{obs} also becomes $[\text{ROOH}]$ -dependent at higher cobalt concentrations (see Figure 2) suggests that the deactivation is somehow

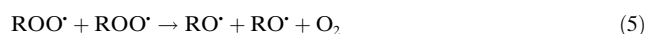
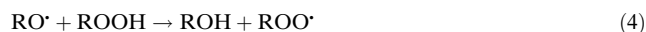
[*] E. Spier, Dr. U. Neuenschwander,^[†] Prof. Dr. I. Hermans
Department of Chemistry and Applied Bio-Sciences ETH Zurich
Wolfgang-Pauli-Strasse 10, 8093 Zurich (Switzerland)
E-mail: hermans@chem.ethz.ch
Homepage: <http://www.hermans.ethz.ch>

[†] Current address: Massachusetts Institute of Technology, Department of Chemical Engineering
77 Massachusetts Avenue, 66-525, Cambridge, MA 02139 (USA)

Supporting information for this article is available on the WWW under <http://dx.doi.org/10.1002/anie.201207920>.

enhanced at higher peroxide concentrations.

Earlier work by our group showed that the alkoxy radicals produced in the reaction of Co^{II} with the hydroperoxide react predominantly with ROOH [Reaction (4)].^[4] The tertiary peroxy radicals in turn, will mainly react with each other producing more alkoxy radicals [Reaction (5)]. Indeed, the fraction of peroxy radicals leading to mutual termination [Reaction (6)] is very small, leading to a radical chain length $\nu \approx 7\text{--}10$. ν is the ratio of the rates of Reactions (5) and (6).^[5]



At low catalyst concentrations, the deperoxidation rate is therefore given by Equation (A) (k_{cat} being the rate constant of the rate-controlling step and $\text{Co}_{\text{active}}$ the active state of the catalyst).^[4]

$$-\text{d}[\text{ROOH}]/\text{d}t = (3 + 2\nu) k_{\text{cat}} [\text{Co}_{\text{active}}] [\text{ROOH}] \quad (\text{A})$$

The observed k_{obs} is hence $(3 + 2\nu)$ times the rate constant of the rate-controlling cobalt-mediated step. In the presence of the radical trap, free radicals are efficiently scavenged, explaining why the observed rate constant decreases by a factor of approximately 10, in agreement with the reported chain length (i.e., $\nu \approx 7\text{--}10$).^[5] Indeed, in the presence of a radical scavenger, one measures purely the ROOH consumption owing to the reactions with the cobalt species. This is valid for $\text{Co}(\text{acac})_2$, as well as $\text{Co}(\text{oct})_2$ (Table 1; see the

Table 1: Experimental Arrhenius expressions for the second-order deperoxidation rate constant in the presence and absence of a radical trap.^[a]

Catalyst	Radical trap	Arrhenius expression
$\text{Co}(\text{acac})_2$	Yes	$2.9 \times 10^9 \text{ M}^{-1} \text{ s}^{-1} \times \exp(-13.0 \text{ kcal mol}^{-1}/RT)$
$\text{Co}(\text{acac})_2$	No	$2.7 \times 10^8 \text{ M}^{-1} \text{ s}^{-1} \times \exp(-12.9 \text{ kcal mol}^{-1}/RT)$
$\text{Co}(\text{oct})_2$	Yes	$1.6 \times 10^{15} \text{ M}^{-1} \text{ s}^{-1} \times \exp(-20.0 \text{ kcal mol}^{-1}/RT)$
$\text{Co}(\text{oct})_2$	No	$1.7 \times 10^{14} \text{ M}^{-1} \text{ s}^{-1} \times \exp(-19.7 \text{ kcal mol}^{-1}/RT)$

[a] Temperature range 30–60 °C; see the Supporting Information.

Supporting Information). The activation energy is not affected by the presence of the bulky and noncoordinating radical trap, in agreement with the assumption that it only reacts with the free radicals.

We emphasize that the Arrhenius expression for the $\text{Co}(\text{acac})_2$ system in the absence of a radical trap is in quantitative agreement with an in situ UV/Vis spectroscopic determination for *tert*-butylhydroperoxide ($1.2 \times 10^{10} \text{ M}^{-1} \text{ s}^{-1} \times \exp(-13 \text{ kcal mol}^{-1}/RT)$; T between 50 and 70 °C).^[4] The expression in the presence of the radical trap agrees very well with the results extracted from the kinetic analysis of the $\text{Co}(\text{acac})_2$ -catalyzed radical formation during α -pinene autoxidation ($3 \times 10^8 \text{ M}^{-1} \text{ s}^{-1} \times \exp(-14 \text{ kcal mol}^{-1}/RT)$; T between 60 and 80 °C).^[6] These results indicate that the precise structure of the peroxide is not crucial.

The prefactor observed for the $\text{Co}(\text{acac})_2$ -catalyzed deperoxidation in the presence of a radical trap ($2.7 \times 10^8 \text{ M}^{-1} \text{ s}^{-1}$) is typical for a bimolecular reaction proceeding via a rather loose transition state. The prefactor obtained for the $\text{Co}(\text{oct})_2$ system in presence of a radical trap ($1.7 \times 10^{14} \text{ M}^{-1} \text{ s}^{-1}$) is however six orders of magnitude larger and points towards a different mechanism. Not only is the preexponential factor significantly different for both catalysts, the Arrhenius activation energy also differs by about 7 kcal mol⁻¹.

To gain more insight, a computational study on the elementary steps of the Fenton reactions [in Reactions (1) and (2)] was performed (Figure 3). Reaction (1) is a typical

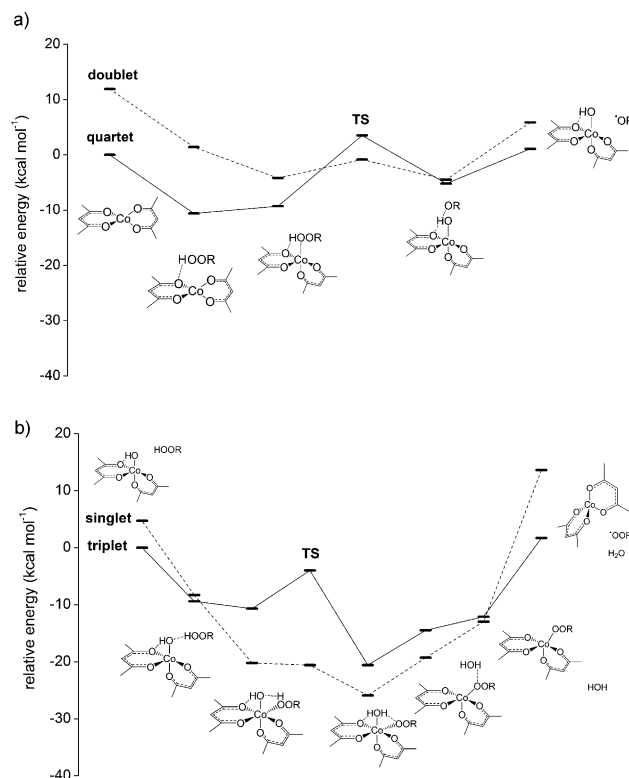
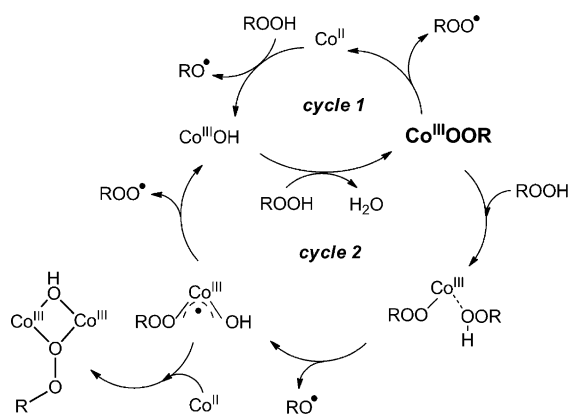


Figure 3. Potential energy diagrams for Reactions (1) (a) and (2) (b) for $\text{Co}(\text{acac})_2$. TS = transition state.

example of two-state reactivity.^[7] While the spin-state with the lowest energy for both the reactants and the products is quartet (in line with recent experimental work),^[8] the lowest transition state is on the doublet energy surface. Whereas a change of the total electronic spin is in principle forbidden, spin-orbit coupling enhances intersystem crossing.^[9] As a consequence, the effective energy barrier of the O–O bond cleavage process is drastically reduced (“spin catalysis”^[7]). The $\text{Co}^{\text{III}}\text{OH}$ species (triplet ground state) react very rapidly with a second ROOH molecule, to $\text{Co}^{\text{III}}\text{OOR}$ which has an almost degenerated singlet/triplet ground state (Figure 3b). These calculations suggest a high $[\text{Co}^{\text{III}}\text{OOR}]/[\text{Co}^{\text{III}}\text{OH}]$ ratio. Dissociation of $\text{Co}^{\text{III}}\text{OOR}$ to ROO^\bullet and the starting Co^{II} species [the reverse reaction for Reaction (3)] proceeds via a variational transition state and

also involves intersystem crossing. This step re-establishes the high-spin ground state of the Co^{II} center. The barrier of this dissociation process is computed to be $14.7 \text{ kcal mol}^{-1}$ for $\text{Co}(\text{acac})_2$. This value is in close agreement with the experimentally observed Arrhenius barrier of 13 kcal mol^{-1} in Table 1. It thus seems plausible that this step is the rate-determining step in the catalytic cycle. Analogous cobalt peroxo species have previously been characterized by X-ray crystallography,^[10] supporting the hypothesis that they are fairly stable. Interestingly, the $\text{Co}^{\text{III}}\text{--OOR}$ bond strength for the $\text{Co}(\text{oct})_2$ complex is predicted to be $20.6 \text{ kcal mol}^{-1}$, which is also in close agreement with the activation energy observed for that system (20 kcal mol^{-1} , see Table 1). However, based on the fact that the preexponential factor for $\text{Co}(\text{oct})_2$ is six orders of magnitude higher than for $\text{Co}(\text{acac})_2$ it seems unlikely that the same step (entropically equivalent) would be rate-controlling. Indeed, this requires a more careful investigation of competing mechanisms.

The unimolecular dissociation of the $\text{Co}^{\text{III}}\text{--OOR}$ complex stands in kinetic competition with the coordination of a ROOH molecule (see Scheme 1). Based on the predicted $\text{Co}^{\text{III}}\text{--OOR}$ bond strengths, we propose that the octoate system will quasi uniquely remain in cycle 2, whereas the acac system will prefer cycle 1.



Scheme 1. Two parallel catalytic cycles, proposed to explain the catalytic deperoxidation of cobalt(II) complexes.

For the octoate system, when keeping to cycle 2, the addition of ROOH to the $\text{Co}^{\text{III}}\text{--OOR}$ complex is followed by O–O bond dissociation (analogous to the first step of the Haber–Weiss cycle). Overall this reaction is exothermic by $5.9 \text{ kcal mol}^{-1}$. In the resulting $\text{Co}^{\text{III}}(\text{OH})(\text{OOR})$ species, one electron spin is distributed over the hydroxyl and peroxy ligands and is hence best described as a cobalt(III) complex with radical ligands, rather than cobalt(IV) with anionic ligands. Dissociation of the ROO• ligand is endothermic by $22.2 \text{ kcal mol}^{-1}$ and regenerates the $\text{Co}^{\text{III}}\text{OH}$ species. We hypothesize that this step is rate-determining for cycle 2, thereby explaining the experimental Arrhenius activation energy of 20 kcal mol^{-1} (see Table 1). As such, the cobalt in the $\text{Co}(\text{oct})_2$ system is overwhelmingly present in the +III oxidation state, and avoids the Co^{II} state. This leads to a very efficient CoOOR/CoOH turnover, thus explaining why the

preexponential factor of the $\text{Co}(\text{oct})_2$ system is about 6×10^5 times higher than for the $\text{Co}(\text{acac})_2$ system (see Table 1).

Regeneration of the $\text{Co}^{\text{III}}\text{OH}$ species stands in kinetic competition with the irreversible formation of a dimer species with free Co^{II} , exothermic for more than 40 kcal mol^{-1} . O–O cleavage in this dimer is very slow, compared with the timescale of the experiment. Dimerization not only lowers the active catalyst concentration, it also reduces the number of radical species. This additional termination reaction leads to a complex cobalt-dependent quasi-steady-state peroxy radical concentration, given by Equation (B).^[11] As the majority of the ROOH is consumed by propagation reaction (5), the deperoxidation rate features a maximum as a function of the cobalt concentration.^[12]

$$[\text{ROO}^\bullet]^2 \approx [\text{Co}] - \text{constant} \times [\text{Co}]^2 \quad (\text{B})$$

In the acac system, the cobalt is predominantly cycling between oxidation states +II and +III. As Co^{II} is required to form the inactive dimer species, more deactivation is observed than for the octoate system, despite the fact that the octoate system is mainly active through cycle 2. However, the competition between cycle 1 and 2 for the acac system is very subtle. Indeed, increasing the $[\text{ROOH}]$ from 20 to 50 mM enhances cycle 2, relative to cycle 1, and leads to more deactivation (Figure 2, curves a and b). Nevertheless, the total cobalt concentration at which this maximum appears remains constant (at ca. $400 \mu\text{M}$).

We conclude that the subtle difference in ligands for the $\text{Co}(\text{acac})_2$ and $\text{Co}(\text{oct})_2$ systems results in a significant difference in $\text{Co}^{\text{III}}\text{--OOR}$ bond strength, inducing very different kinetic behavior.

In an attempt to minimize the deactivation through the formation of inactive dimers, we aimed at synthesizing a site-isolated heterogeneous cobalt catalyst. Indeed, attaching the active Co^{II} sites to an alumina support would prevent dimerization and facilitate catalyst recycling. Various amounts of $\text{Co}(\text{NO}_3)_2$ were impregnated on γ -alumina and calcined at 500°C . For a Co loading of 0.75 w %, no evidence for cobalt oxide nanoparticles could be obtained with Raman spectroscopy. A narrow UV absorption below 300 nm and a typical triplet feature in the visible region confirm the predominant presence of tetrahedral Co^{II} (see the Supporting Information). In contrast to the homogeneous complexes, no sign of catalyst deactivation could be observed for this solid catalyst (see Figure 1, curve c). Indeed, full deperoxidation can be achieved with this heterogeneous analogue. No blank activity was observed for pure Al_2O_3 (see the Supporting Information).

When studying different cobalt concentrations by adding more and more catalyst to the reactor, no maximum in k_{obs} could be obtained (Figure 4, curve b). Instead, perfect first-order behavior in cobalt was observed up to $600 \mu\text{M}$. A hot separation test confirmed the heterogeneous nature of the catalysis;^[13] when removing the solid catalyst at reaction temperature, the activity of the supernatant indeed drops to zero (see the Supporting Information). This is rather remarkable, as many analogous catalysts were found to slowly leach active species into solution, thereby causing actually homo-

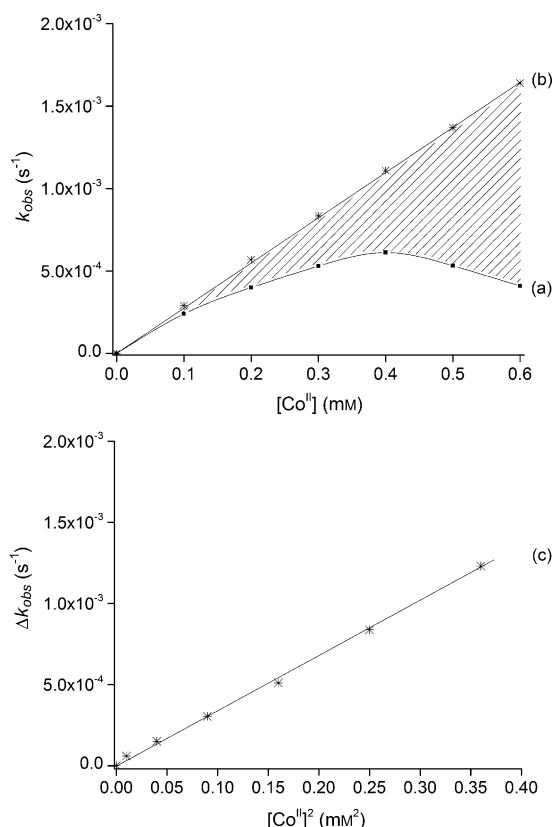


Figure 4. Pseudo first-order deperoxidation rate constant k_{obs} at 40 °C as a function of the cobalt concentration for $\text{Co}(\text{acac})_3$ (a) and the heterogeneous 0.75 wt % $\text{Co}/\text{Al}_2\text{O}_3$ (b); c) difference between the activity of the heterogeneous and homogeneous systems (highlighted area in the top panel) reveals second-order behavior in $[\text{Co}^{\text{II}}]$.

geneous catalysis.^[13] We emphasize that the difference between k_{obs} obtained for the heterogeneous catalyst and the homogeneous $\text{Co}(\text{acac})_3$ system shows perfect second-order behavior with respect to the cobalt concentration (curve c in Figure 4). This observation supports our hypothesis that the deactivation of the homogeneous catalytic systems is related to the formation of inactive dimers as outlined above [see for example, Equation (B)]. As such, we used a heterogeneous catalyst to verify a hypothesis for the homogeneous systems. The comparison of the Arrhenius expression obtained for the 0.75 wt % $\text{Co}/\text{Al}_2\text{O}_3$, that is, $k(T) = 6.5 \times 10^{12} \text{ M}^{-1} \text{ s}^{-1} \times \exp(-20.7 \text{ kcal mol}^{-1}/RT)$, with that for $\text{Co}(\text{acac})_3$ in Table 1 suggests that this solid catalyst also operates mainly through cycle 2 (see Scheme 1). The reason why the preexponential factor is 250 times smaller for the heterogeneous system can be ascribed to steric congestion by the solid support, hindering substrate approach.

In conclusion, cobalt complexes homolytically activate alkyl hydroperoxides. Subtle differences in the ligands can result in extreme differences in the catalytic cycles, either leading to an active and stable catalyst, or a catalyst that quickly deactivates owing to the formation of inactive dimers. Immobilization of cobalt on alumina results in a heterogeneous catalyst that is not subject to leaching nor to deactivation, as dimerization is prohibited.

Experimental Section

Deperoxidation experiments were carried out in a 50 mL glass reactor. 15 mL of catalyst solution (predistilled cyclohexane solvent) was heated to reaction temperature in an oil bath, prior to the addition of cumyl hydroperoxide (20 mM, unless otherwise stated). Samples (120 μL) were taken at regular intervals and diluted in acetic acid (15 mL). Excess of a KI solution was added under N_2 bubbling. After 15 min, a back titration was performed under inert conditions, by using a sodium thiosulfate solution. The average of three titrations was used in the kinetic analysis. As cobalt(II) complexes we used cobalt(II) acetylacetonate (Acros Organics, 99%) and cobalt(II) octoate (i.e., cobalt(II) 2-ethylhexanoate, Aldrich 65 wt % in mineral spirits).

Quantum chemical calculations were performed with the Gaussian09 software,^[14] using Truhlar's M06-L functional^[15] and taking into account solvent effects (cyclohexane) with the Polarizable Continuum Model.^[16] The geometry was optimized by using the 6-31G(d,p) basis set; the energy was further refined by performing a single point calculation using the 6-311++G(df,pd) basis set. For cobalt, an f-polarized Los Alamos Effective Core Potential basis set (LANL2DZ(f))^[17] was used in the geometry optimization and single point calculations. The reported relative energies of the stationary points on the adiabatic potential energy surfaces (the energy barriers E_b and reaction energies $\Delta_r E$) were corrected for zero-point-energy (ZPE) differences. The ligands of the $\text{Co}(\text{oct})_2$ complex were simplified by isobutyrate ligands for computational convenience.

Received: October 1, 2012

Revised: November 16, 2012

Published online: December 17, 2012

Keywords: catalyst deactivation · heterogeneous catalysis · homogeneous catalysis · kinetics · selective oxidation

- [1] R. A. Sheldon, J. K. Kochi, *Metal Catalyzed Oxidations of Organic Compounds*, Academic Press, New York, **1981**.
- [2] I. Hermans, J. Peeters, P. A. Jacobs, *Top. Catal.* **2008**, *50*, 124.
- [3] I. Hermans, P. A. Jacobs, J. Peeters, *Chem. Eur. J.* **2007**, *13*, 754.
- [4] N. Turrà, U. Neuenschwander, A. Baiker, J. Peeters, I. Hermans, *Chem. Eur. J.* **2010**, *16*, 13226.
- [5] R. Hiatt, J. Clipsham, T. Visser, *Can. J. Chem.* **1964**, *42*, 2754.
- [6] U. Neuenschwander, I. Hermans, *J. Catal.* **2012**, *287*, 1.
- [7] a) D. K. Böhme, H. Schwarz, *Angew. Chem.* **2005**, *117*, 2388; *Angew. Chem. Int. Ed.* **2005**, *44*, 2336; b) R. Poli, J. N. Harvey, *Chem. soc. Rev.* **2003**, *32*, 1; c) J. N. Harvey, R. Poli, K. M. Smith, *Coord. Chem. Rev.* **2003**, *238–239*, 347; d) D. Schröder, S. Shaik, H. Schwarz, *Acc. Chem. Res.* **2000**, *33*, 139.
- [8] P. Pietrzyk, M. Srebro, M. Radon, Z. Sojka, A. Michalak, *J. Phys. Chem. A* **2011**, *115*, 2316.
- [9] As expected, spin-orbit coupling was found to be important for cobalt (complexes); see for example: a) M. Vijayakumar, M. S. Gopinathan, *J. Mol. Struct. (Theochem)* **1996**, *361*, 15; b) C. N. Sakellaris, A. Mavridis, *J. Phys. Chem. A* **2012**, *116*, 6935; c) A. M. Bryan, W. A. Merrill, W. M. Reiff, J. C. Fetting, P. P. Power, *Inorg. Chem.* **2012**, *51*, 3366.
- [10] a) F. A. Chavez, J. M. Rowland, M. M. Olmstead, P. K. Mascharak, *J. Am. Chem. Soc.* **1998**, *120*, 9015; b) F. A. Chavez, J. A. Briones, M. M. Olmstead, P. K. Mascharak, *Inorg. Chem.* **1999**, *38*, 1603.
- [11] Rate of initiation $R_{\text{init}} = k_{\text{cat}}[\text{Co}^{\text{active}}][\text{ROOH}]$; rate of termination $R_{\text{term}} = 2k_6[\text{ROO}^\bullet]^2 + 2k_{\text{dimer}}[\text{Co}^{\text{III}}(\text{OH})(\text{OOR})][\text{Co}^{\text{II}}]$. Under quasi-steady-state (QSS) conditions, $R_{\text{init}} = R_{\text{term}}$, leading to Equation (B) for the QSS peroxy radical concentration.
- [12] This implies the assumption of fast interconversion (seconds timescale) of the Co^{II} , $\text{Co}^{\text{III}}\text{OH}$, $\text{Co}^{\text{III}}\text{OOR}$, and $\text{Co}^{\text{III}}(\text{OH})$.

- (OOR) species, such that the initially observed k_{obs} is affected by dimerization of $\text{Co}^{\text{III}}(\text{OH})(\text{OOR})$ plus Co^{II} . This hypothesis seems reasonable, given the low interconversion barriers and the fairly high peroxide concentration.
- [13] R. A. Sheldon, M. Wallau, I. W. C. E. Arends, U. Schuchardt, *Acc. Chem. Res.* **1998**, *31*, 485.
- [14] Gaussian09, Revision A.02, M. J. Frisch et al., Gaussian, Inc., Wallingford CT, **2009**. See the Supporting Information.
- [15] a) R. Valero, R. Costa, I. P. R. Moreira, D. G. Truhlar, F. Illas, *J. Chem. Phys.* **2008**, *128*, 114103; b) Y. Zhao, D. G. Truhlar, *Acc. Chem. Res.* **2008**, *41*, 157.
- [16] J. Tomasi, B. Mennucci, R. Cammi, *Chem. Rev.* **2005**, *105*, 2999.
- [17] A. W. Ehlers, M. Nöhme, S. Dapprich, A. Gobbi, A. Höllwarth, V. Jonas, K. F. Köhler, R. Stegmann, A. Veldkamp, G. Frenking, *Chem. Phys. Lett.* **1993**, *208*, 111.
-